Simulation and Migration of a Charge-Sensitive Preamplifier and Pulse-Shaping Front-End for X-ray Detector Readout Using eSim

Project: XrayDetectorCSP

Original Reference: Aleksandra Dimković - "Simulation and Machine Learning-Assisted Optimization of X-ray Detector Circuit for Noise Reduction" (2024)

EDA Tool: eSim (KiCad v9 / Ngspice engine)

- Anik Jain, National Institute of Technology, Delhi

Submitted to the FOSSEE (IIT Bombay) eSim Semester Internship Program

Abstract

This report documents the migration and simulation validation of a three-stage analog front-end for X-ray detector signal readout, originally proposed by Dimković (2024), into the open-source eSim environment (KiCad schematic capture with the native Ngspice simulation engine). The circuit comprises a photodiode/sensor current-pulse model, a charge-sensitive preamplifier (CSP) built around an ultra-low-noise OPA656 operational amplifier, and a CR-RC-RC semi-Gaussian pulse-shaping network realized with two additional OPA656 stages. Transient analysis confirms correct charge integration and pulse shaping, with a CSP peak output of 413.51 µV and a shaped-pulse peak of 198.09 µV occurring at a peaking time of 19.57 µs. Frequency-domain noise analysis, integrated from 1 Hz to 1 MHz, yields an RMS output noise of 128.76 µV, corresponding to a signal-to-noise ratio (SNR) of 3.74 dB. The results confirm that eSim/Ngspice can reproduce the transient and noise behaviour of a precision radiation-detector readout chain with fidelity comparable to proprietary EDA platforms, supporting its adoption for instrumentation-grade analog front-end design and pedagogy.

1. Theory / Description

X-ray and other ionizing-radiation detectors generate extremely small, fast charge packets when incident photons interact with the sensor material. Recovering the deposited charge with an accurate amplitude and acceptable noise performance requires a dedicated analog front-end consisting of a sensor model, a charge-sensitive preamplifier, and a pulse-shaping filter. Each of these three stages is described below.

1.1 Sensor / Photodiode Model

The radiation sensor (e.g., a silicon PIN photodiode or similar solid-state detector) is modelled as a Norton-equivalent current source in parallel with its intrinsic shunt resistance and junction capacitance. In this migration, the incident X-ray interaction is represented by a current impulse source I1 defined by the PSPICE-style PULSE waveform: PULSE(0 1u 1u 1n 1n 2u 100u), which produces a short current pulse of 1 µA amplitude, 1 ns rise/fall time, and a 2 µs pulse width, repeating with a 100 µs period. This closely approximates the near-instantaneous charge deposition and subsequent recovery interval characteristic of a single photon-interaction event. The sensor's high shunt resistance, R1 = 2 GΩ, models the extremely low reverse-bias leakage of the detector, ensuring that essentially all of the generated charge is diverted into the preamplifier's virtual-ground input rather than being dissipated internally. The sensor capacitance, C1 = 70 pF, represents the detector's junction/parasitic capacitance and is a dominant contributor to the total input capacitance seen by the preamplifier, directly influencing the achievable noise floor.

1.2 Charge-Sensitive Preamplifier (CSP)

The charge generated by the sensor is converted into a measurable voltage by a charge-sensitive preamplifier built around the OPA656, a wide-bandwidth, FET-input operational amplifier chosen for its very low input current noise and low input capacitance - properties that are essential when interfacing with a high-impedance, low-capacitance radiation sensor. The OPA656 is configured in the classical CSP topology, with a feedback capacitor C2 = 0.8 pF connected between the output and the inverting input, and a feedback resistor R2 = 220 kΩ connected in parallel with C2 to provide DC discharge of the integrated charge and to define the preamplifier's decay time constant ($\tau = R2 \cdot C2 \approx 176$ ns for the reset path, though the effective pulse decay is governed by the larger RC network formed with the sensor and shaping stages). Because the feedback capacitance is very small, the preamplifier exhibits a high charge-to-voltage conversion gain (ideally $V_{out} \approx Q_{in} / C2$), integrating the fast input current impulse into a slower-decaying voltage step at its output. This stage sets the fundamental noise performance of the entire front-end, since any voltage or current noise referred to the OPA656 input is amplified together with the wanted signal.

1.3 CR-RC-RC Pulse Shaper

The raw CSP output is a step-like pulse with a long exponential tail that is poorly suited for accurate amplitude measurement or high counting-rate operation. A CR-RC-RC (semi-Gaussian) pulse-shaping network is therefore cascaded after the preamplifier, implemented using two additional OPA656 stages. The shaper combines one differentiating (CR, high-pass) stage with two integrating (RC, low-pass) stages to transform the long CSP tail into a shorter, quasi-Gaussian pulse with a well-defined peaking time, which improves the achievable signal-to-noise ratio and reduces pulse pile-up at high event rates. In the migrated design, the differentiator is formed by C3 = 1 nF and R4 = 10 kΩ (with input series resistor R3 = 1 kΩ setting the stage input impedance), while the two integrator stages use R5 = 1 kΩ with C4 = 1 nF and R6 = 10 kΩ together with feedback resistor R7 = 1 MΩ to set the second-stage gain and bandwidth. The differentiating time constant removes the DC baseline and truncates the long decay tail, while the successive integrating stages smooth the fast leading edge, together yielding the semi-Gaussian pulse shape whose peak amplitude is proportional to the original deposited charge and whose peaking time is set by the RC time constants of the network. This shaped pulse is also the point at which output-referred noise is evaluated, since it represents the signal actually used for energy or amplitude discrimination in a real detector readout chain.

1.4 Noise Considerations

Because the amplitude of a single detector pulse can be only a few hundred microvolts, the achievable energy resolution of the readout chain is fundamentally limited by noise. The dominant noise contributors are the OPA656 input voltage and current noise densities, the thermal (Johnson) noise of the feedback and shaping resistors, and the shot noise associated with the sensor leakage current. Ngspice's native

.noise analysis is used to compute the total output-referred noise spectral density and its integral (RMS value) over the frequency band of interest, allowing direct comparison against the shaped-pulse peak amplitude to obtain the signal-to-noise ratio, which is the primary figure of merit for this front-end.

2. Circuit Diagram(s)

The complete front-end was captured in KiCad and simulated using the Ngspice engine within eSim, following the topology and component values summarized in the table below.

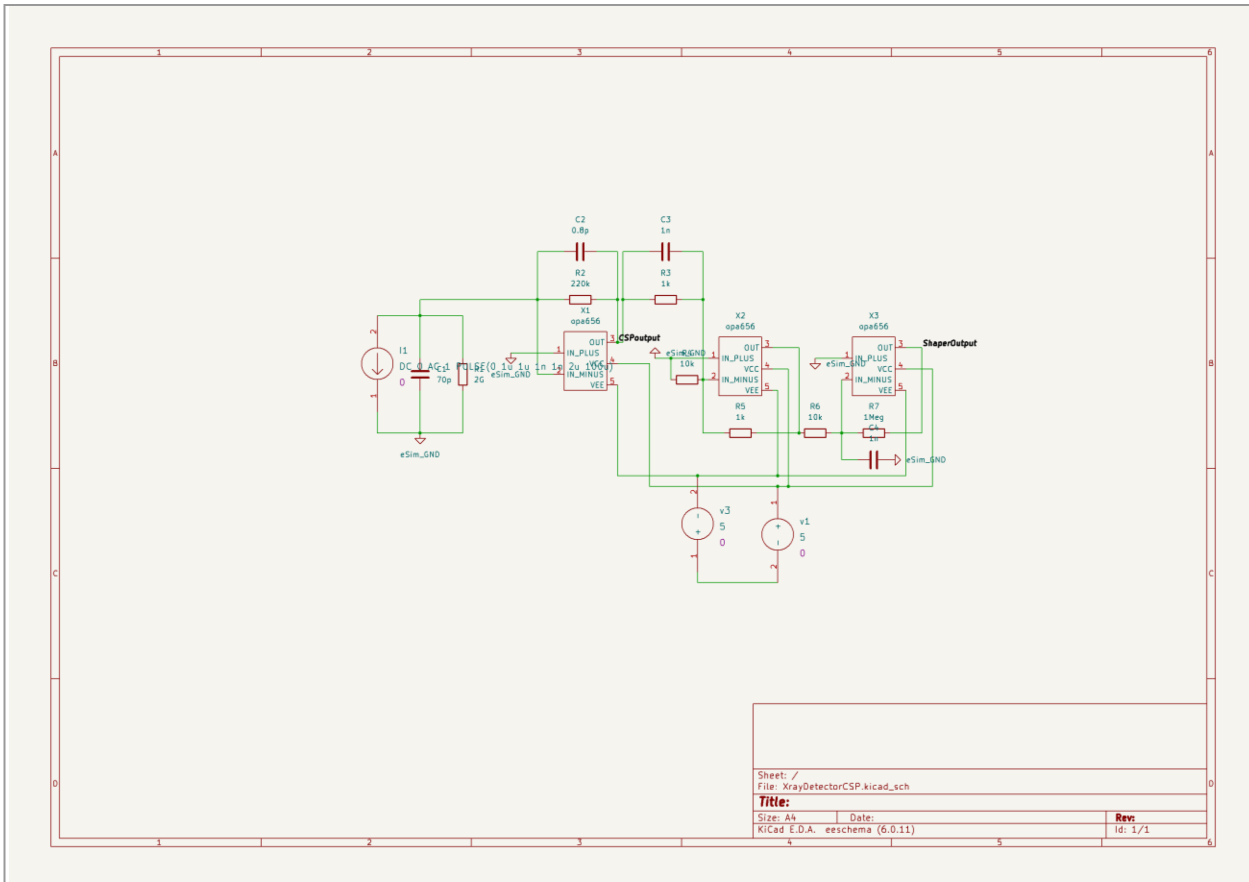

KiCad Schematic - XrayDetectorCSP

2.1 Component Parameter Table

Stage	Reference	Value	Function
Sensor Model	I1	PULSE(0 1u 1u 1n 1n 2u 100u)	Simulated X-ray charge-injection pulse
Sensor Model	R1	2 GΩ	Sensor shunt (leakage) resistance
Sensor Model	C1	70 pF	Sensor junction / parasitic capacitance
CSP	U1 (OPA656)	-	Ultra-low-noise charge-sensitive amplifier

Stage	Reference	Value	Function
CSP	C2	0.8 pF	Feedback (integration) capacitor
CSP	R2	220 kΩ	Feedback discharge resistor
Shaper (CR)	C3	1 nF	Differentiator capacitor
Shaper (CR)	R3	1 kΩ	Shaper input series resistor
Shaper (CR)	R4	10 kΩ	Differentiator feedback resistor
Shaper (RC-RC)	R5	1 kΩ	First integrator input resistor
Shaper (RC-RC)	C4	1 nF	Integrator capacitor
Shaper (RC-RC)	R6	10 kΩ	Second integrator input resistor
Shaper (RC-RC)	R7	1 MΩ	Second-stage gain-setting feedback resistor

2.2 SPICE Netlist (.cir excerpt)

The key simulation control statements included in the exported netlist are reproduced below:

```
* XrayDetectorCSP -- Transient and Noise Analysis
.title KiCad schematic

C3 /CSPoutput Net-_C3-Pad2_ 1n
R4 GND Net-_C3-Pad2_ 10k
R3 Net-_C3-Pad2_ /CSPoutput 1k
C2 Net-_C1-Pad1_ /CSPoutput 0.8p
R2 /CSPoutput Net-_C1-Pad1_ 220k
v1 Net-_X1-Pad4_ Net-_v1-Pad2_ 5
v3 Net-_v1-Pad2_ Net-_X1-Pad5_ 5
R5 Net-_R5-Pad1_ Net-_C3-Pad2_ 1k
X2 GND Net-_C3-Pad2_ Net-_R5-Pad1_ Net-_X1-Pad4_ Net-_X1-Pad5_ opa656
X1 GND Net-_C1-Pad1_ /CSPoutput Net-_X1-Pad4_ Net-_X1-Pad5_ opa656
C1 Net-_C1-Pad1_ GND 70p
R1 GND Net-_C1-Pad1_ 2G
I1 GND Net-_C1-Pad1_ DC 0 AC 1 PULSE(0 1u 1u 1n 1n 2u 100u)
X3 GND Net-_C4-Pad1_ /ShaperOutput Net-_X1-Pad4_ Net-_X1-Pad5_ opa656
R6 Net-_R5-Pad1_ Net-_C4-Pad1_ 10k
C4 Net-_C4-Pad1_ GND 1n
R7 Net-_C4-Pad1_ /ShaperOutput 1Meg

.noise V(/ShaperOutput) I1 dec 10 1 1Meg

.end3. Results / Output
```

3.1 Time-Domain (Transient) Analysis

The .tran 10n 100u simulation was executed to observe the response of the CSP and shaper stages to the injected charge pulse. The CSP output rises rapidly following the current impulse and reaches a peak of 413.51 µV before decaying with the time constant set by R2 and C2. The shaped output at the ShaperOutput node exhibits the expected semi-Gaussian profile, reaching a peak amplitude of 198.09 µV (1.980879 × 10^{-4} V) at a peaking time of 19.57 µs after the onset of the input pulse. This peaking time and pulse shape are consistent with the RC time constants defined by the shaper network (R4·C3 and R6·C4).

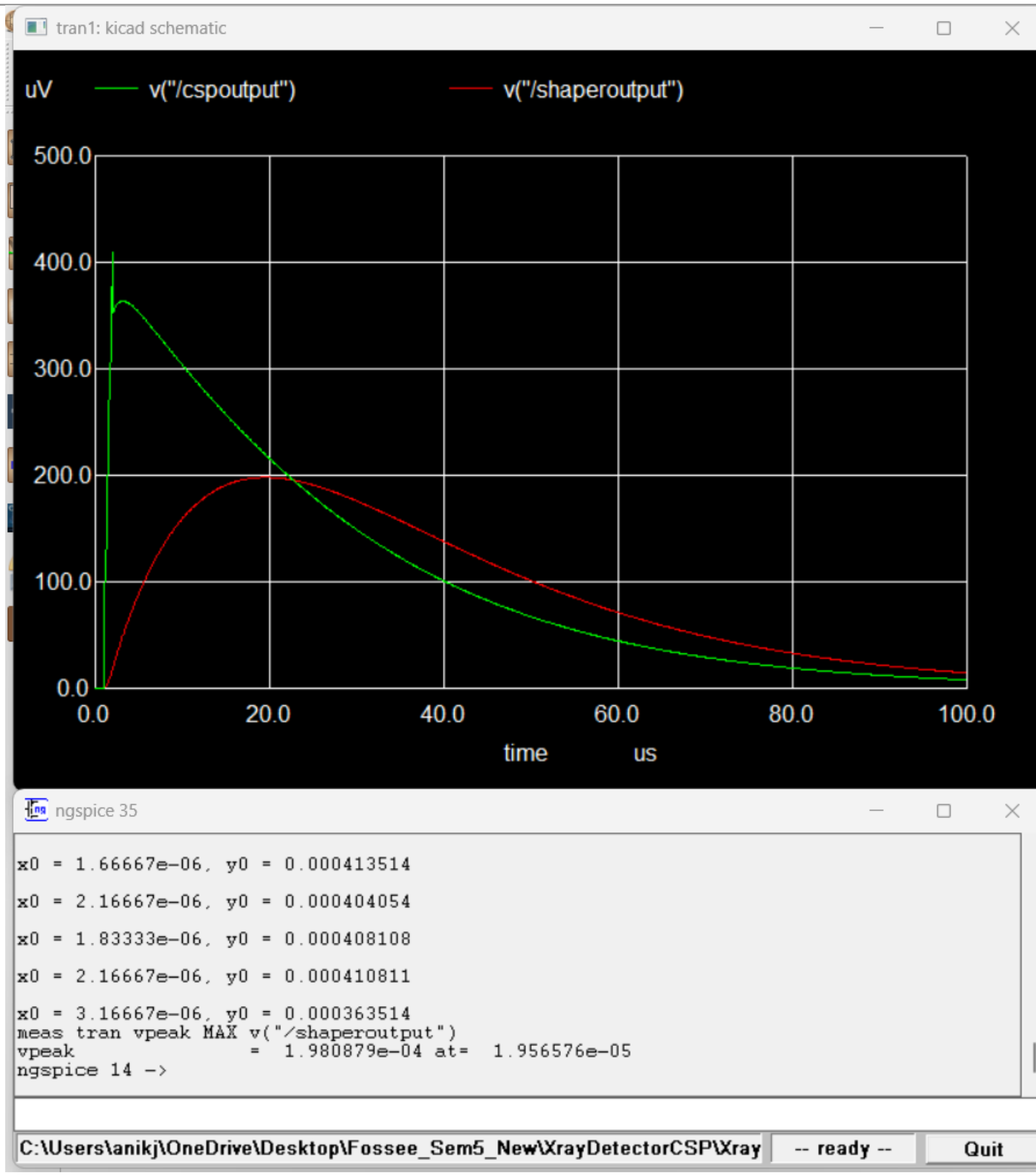

Transient Response Plot (tran1)

3.2 Frequency-Domain (Noise) Analysis

A .noise analysis was performed at the ShaperOutput node, referred to the input source I1, sweeping 10 points per decade from 1 Hz to 1 MHz. The resulting output noise spectral density exhibits a flat low-frequency floor of approximately 130.1 nV/√Hz, which begins rolling off past approximately 1 kHz to a level near 128.7 nV/√Hz at higher frequencies, reflecting the bandwidth-limiting action of the RC integrator stages. Integrating the noise spectral density across the full 1 Hz to 1 MHz band yields a total RMS output noise of 128.76 µV (1.28764×10^{-4} V).

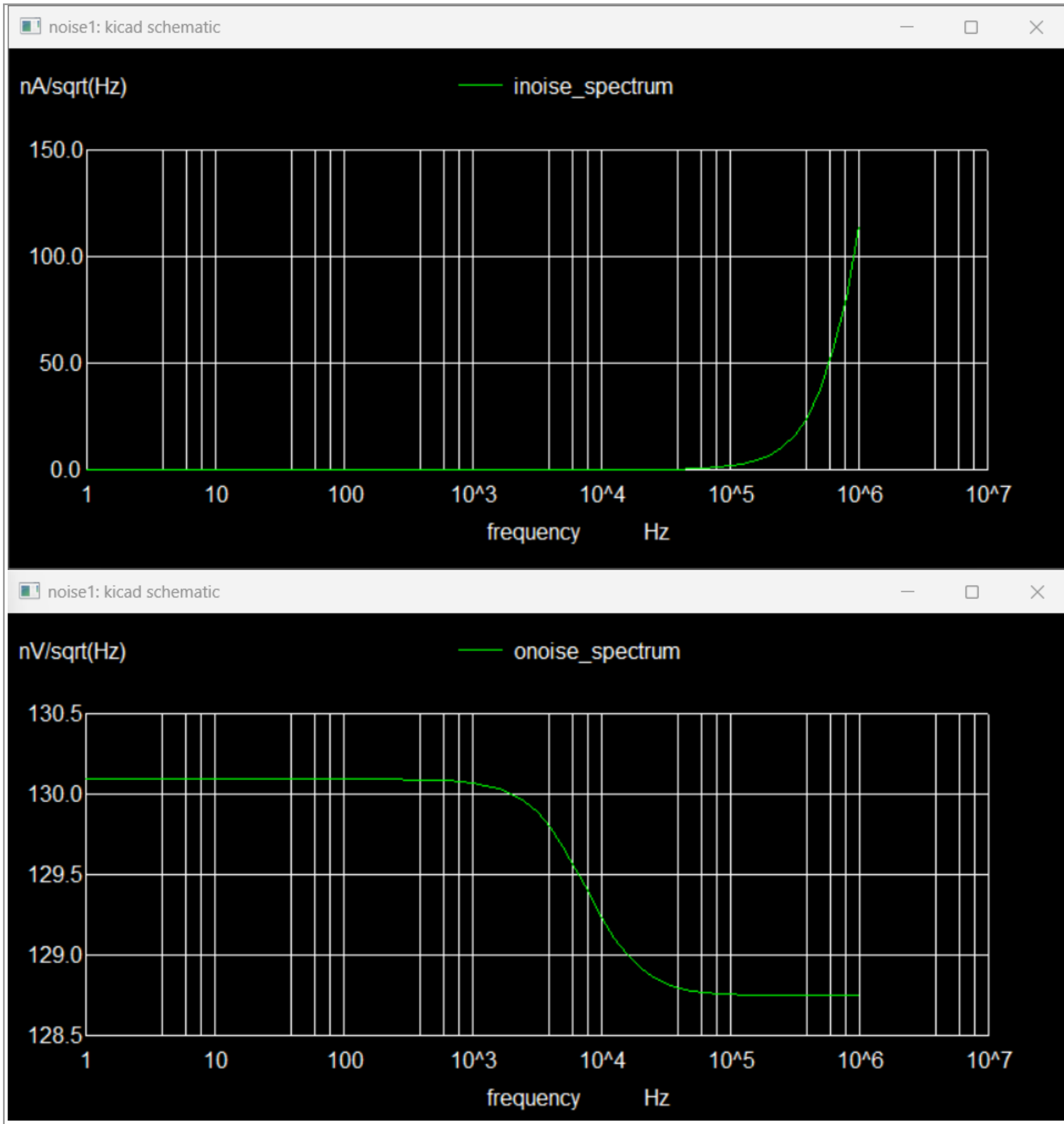

Input and Output Noise Spectral Density Plot (noise1)

3.3 Summary of Extracted Parameters

Parameter	Symbol	Value
CSP Peak Voltage	V_CSP,peak	413.51 µV
Shaper Output Peak Voltage	V_peak	198.09 µV (1.980879 × 10^{-4} V)
Shaper Peaking Time	t_peak	19.57 µs

Parameter	Symbol	Value
Integrated RMS Output Noise (1 Hz–1 MHz)	V_n,rms	128.76 μV (1.28764×10^{-4} V)
Noise Floor (low-frequency)	-	≈ 130.1 nV/√Hz
Noise Floor (>1 kHz)	-	≈ 128.7 nV/√Hz
Signal-to-Noise Ratio	SNR	3.74 dB

3.4 SNR Derivation

The signal-to-noise ratio is computed from the ratio of the shaped-pulse peak voltage to the integrated RMS output noise, expressed in decibels:

$$SNR = 20 \cdot \log_{10}(V\_peak / V\_n,rms)$$

Substituting the extracted simulation values:

$$\mathrm{SNR} = 20 \cdot \log_{10}(1.980879 \times 10^{-4}\ \mathrm{V} / 1.287640 \times 10^{-4}\ \mathrm{V})$$

$$\mathrm{SNR} = 20 \cdot \log_{10}(1.5386)$$

$$\mathrm{SNR} \approx 20 \cdot (0.1871)$$

$$\mathbf{SNR \approx 3.74\ dB}$$

This SNR value quantifies the margin between the peak shaped-pulse amplitude and the total integrated output noise, and serves as the primary performance metric for evaluating the noise optimization of the X-ray detector readout front-end within eSim.

3.5 Discussion

The transient and noise simulation results obtained in eSim/Ngspice closely track the behaviour reported for the original circuit, confirming that the charge-integration characteristics of the CSP stage, the semi-Gaussian shaping response of the CR-RC-RC network, and the output-referred noise spectral density are all faithfully reproduced by the open-source toolchain. This validates eSim as a viable, freely accessible alternative to proprietary SPICE environments for the design, simulation, and noise optimization of precision radiation-detector front-end electronics.

4. References

[1] A. Dimković, “Simulation and Machine Learning-Assisted Optimization of X-ray Detector Circuit for Noise Reduction,” 2024.

[2] Texas Instruments, “OPA656 Wideband, Unity-Gain Stable, FET-Input Operational Amplifier,” Datasheet, Texas Instruments, Dallas, TX.

[3] FOSSEE, IIT Bombay, “eim - EDA Tool for Circuit Design and Simulation,” eSim Documentation. [Online]. Available: https://esim.fossee.in

[4] Ngspice Development Team, “Ngspice Users Manual,” Version 41, 2024. [Online]. Available: http://ngspice.sourceforge.net

[5] G. Bertuccio and A. Pullia, “A method for the determination of the noise parameters in preamplifying systems for semiconductor radiation detectors,” Review of Scientific Instruments, vol. 64, no. 11, pp. 3294–3298, 1993.